"Physics of Auroral Phenomena", Proc. XLIV Annual Seminar, Apatity, pp. 100-106, 2021

Polar
Geophysical
Institute

DOI: 10.51981/2588-0039.2021.44.023

ESTABLISHING SOLAR ACTIVITY TREND FOR SOLAR CYCLES 21 – 24

A.K. Singh* and A. Bhargawa

**Physics Department, University of Lucknow, Lucknow-226 007, India;* e-mail: *aksphys@gmail.com*

Abstract. Solar-terrestrial environment is manifested primarily by the physical conditions of solar interior, solar atmosphere and eruptive solar plasma. Each parameter gives unique information about the Sun and its activity according to its defined characteristics. Hence the variability of solar parameters is of interest from the point of view of plasma dynamics on the Sun and in the interplanetary space as well as for the solar-terrestrial physics. In this study, we have analysed various solar transients and parameters to establish the recent trends of solar activity during solar cycles 21, 22, 23 and 24. The correlation coefficients of linear regression of F10.7 cm index, Lyman alpha index, Mg II index, cosmic ray intensity, number of M & X class flares and coronal mass ejections (CMEs) occurrence rate versus sunspot number was examined for last four solar cycles. A running cross-correlation method has been used to study the momentary relationship among the above mentioned solar activity parameters. Solar cycle 21 witnessed the highest value of correlation for F10.7 cm index, Lyman alpha index and number of M-class and X-class flares versus sunspot number among all the considered solar cycles which were 0.979, 0.935 and 0.964 respectively. Solar cycle 22 recorded the highest correlation in case of Mg II index, Ap index and CMEs occurrence rate versus sunspot number among all the considered solar cycles (0.964, 0.384 and 0.972 respectively). Solar cycle 23 and 24 did not witness any highest correlation compared to solar cycle 21 and 22. Further the record values (highest value compared to other solar three cycles) of each solar activity parameters for each of the four solar cycles have been studied. Here solar cycle 24 has no record text at all, this simply indicating that this cycle was a weakest cycle compared to the three previous ones. We have concluded that in every domain solar 24 was weaker to its three predecessors.

Keywords: Solar cycles; Solar activity; Sunspot numbers; Solar transients.

1. Introduction

In order to study the characteristic features of solar activity, we need to have some suitable parameters that can be used to depict the various forms of solar output. Several features of solar activity considering different indices have been studied on the basis of two major distinctions between them (*White et al.*, 1998; *Goode and Pallé*, 2007; *Kopp and Lean*, 2011; *Singh and Tonk*, 2014; *Singh and Bhargawa*, 2017; 2019; 2020; *Bhargawa and Singh*, 2021). First aspect deals with the frequency time aspect of solar activity involving the consideration of a set of time variation in different solar activity indices. The second one is spatial aspect which implies the study of spatial distribution of solar activity phenomena and degree of homogeneity or inhomogeneity in the characteristic features of solar activity indices according to their heliographical position (*Goode and Pallé*, 2007; *Turner et al.*, 2013).

Variety of solar activity phenomena represented by various indices is coded in a compact numerical form (*DeLand and Cebula*, 1994). These indices are classified in different ways and can be subdivided into basic physical indices and derived indices. Basic indices represent numerical characteristics of solar activity observed and measured directly such as; sunspot numbers, sunspot area, flare brightness etc (*Egorova et al.*, 2004). All other indices are derived from the processing of basic indices or their combinations, for example, Wolf number, flare indices, fluctuation indices, etc (*Roeckner et al.*, 2006). Thus, the indices for which determination and computation of active region area, lifetime, and intensities that are considered will predominantly reflect the behaviour of these indices. Frequency indices represent the similar number of observed active region formations during specified period (*Egorova et al.*, 2004).

Space weather indices include sunspot number, geomagnetic indices, solar wind parameters (density and speed), flare index, solar x-ray flux and many more (*Papaioannou et al.*, 2016). As our knowledge of space weather progresses new indices will undoubtedly arise and old indices will be consolidated. Two of the most used space weather indices are smoothed sunspot number (SSN) and the geomagnetic planetary A index (Ap) (*Menvielle et al.*, 2011). The other most important solar index is solar ten centimetre radio flux (F10.7). This is closely related to SSN. Both SSN and F10.7 give an indication of the overall level of solar activity (*Hanuise et al.*, 2006). SSN ranges from zero to over 300. Although this value is said to indicate solar activity, it does not always mean activity with regard to flares and coronal mass ejections (*Gaidash et al.*, 2017). It might be regarded as similar to a space weather temperature, but we must be careful with such analogies. The Ap index, and its logarithmic cousin Kp, give a measure of the storminess of the Earth's magnetic field (*Menvielle at al.*, 2011; *Gulyaeva and Gulyaev*, 2020).

In the present paper, we have attempted to study the relative merits of various solar indices (F10.7 cm flux, Lyman alpha index, Mg II index, cosmic ray intensity and Ap index) in relation to SSN and their interrelationship. The observed peculiarities/abnormalities, particularly in the relationship between SSN and solar flare / coronal mass ejection have also been discussed. It is quite new approach to analyze and correlate the characteristic features of different solar activity parameters in relation to sunspot numbers.

2. Data sources

The time series data for sunspot number (version 2), F10.7 cm flux (F10.7 index), Lyman alpha index, Dst index, proton events and Ap index are taken from NASA's Space Physics Data Facility website (https://spdf.gsfc.nasa.gov). Mg II index data are taken from LASP Interactive Solar Data centre (http://lasp.colorado.edu). The Cosmic ray intensity and Ground Level Enhancements (GLE) data has been adopted from Cosmic Ray Station of the University of Oulu (https://cosmicrays.oulu.fi). The solar flare data are taken from the NOAA`s website (fttp://fttp.ngdc.noaa.gov/STP/SOLAR_DATA) available in public domain and the CMEs occurrence data has been taken from ARTEMIS catalogue (http://cesam.lam.fr/lascomission/ARTEMIS/). All the considered time series data of different solar parameters covers the time period of four recently observed solar cycles 23&24.

3. Results and discussion

Solar cycle 24 has already approached its minimum and many studies have declared it the weakest cycle since past 100 years (*Singh and Bhargawa*, 2017, 2019; *Pesnell*, 2020). In the present study solar cycle 24 has been compared to the three previous cycles (solar cycle 21, 22 and 23) covering more than 40 year’s data in total. The solar cycles are evaluated on the basis of highest and lowest activity periods, the correlation between the parameters and the record values of solar parameters. The parameters used in this analysis include the sunspot number, the 10.7 cm radio flux, the number of extreme solar flares (X-class flares), proton events (particle energy $\geq$ 10 MeV), Ground Level Enhancements (GLE), and geomagnetic indices such as Kp and Ap indices which are the measure of geomagnetism. To compare this poor performance of solar cycle 24 (SC24) to the previous solar cycles 21-23, we have used the famous NOAA-scales which link objective solar parameters such as the x-ray flux to all kinds of practical space weather effects such as on radio communication.

Table 1. Different level of solar events: radio blackouts (R-scale), solar radiation storms (S-scale) and geomagnetic storms (G-scale).

Level	Radio blackouts		Proton storms		Geomagnetic storms	
	Scale	X-ray	Scale	Pfu*	Scale	Kp
Extreme	R5	X20	S5	100000	G5	9
Severe	R4	X10	S4	10000	G4	8
Strong	R3	X1	S3	1000	G3	7
Moderate	R2	M5	S2	100	G2	6
Minor	R1	M1	S1	10	G1	5

The scales given in table 1 describe three types of environmental disturbances: radio blackouts (R-scale), solar radiation storms (S-scale) and geomagnetic storms (G-scale). For these, three physical parameters have been used respectively: solar flares (x-ray flux), proton storms (pfu: particle flux unit; number of protons with energies greater than 10 MeV), and the Kp-index. All scales consists of 5 levels (1 to 5), conveying the intensity of the event (minor to extreme). Table 1 provides a summary of scales and intensities. For example, an X 6.9 flare would be rated as an R3 event, a proton flare with a peak flux of e.g. 350 pfu would be rated as an S2 event (between 100 and 1000 pfu), and a severe geomagnetic storm (Kp=8) as a G4 event.

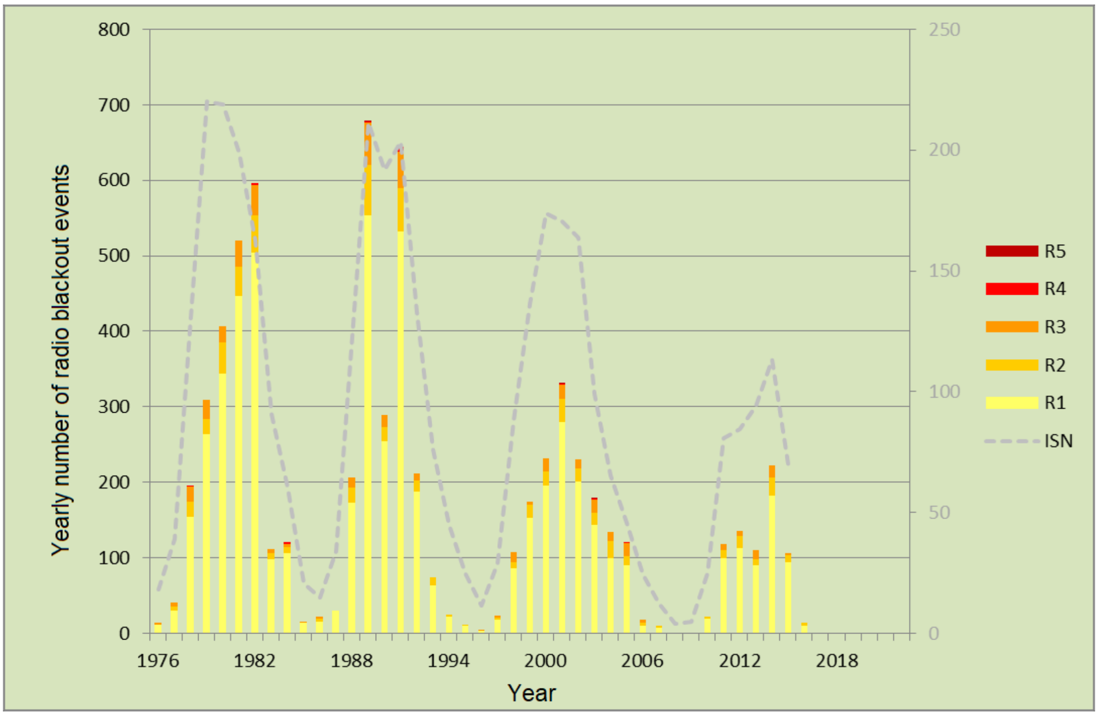

Figure 1. Number of radio blackout events during solar cycles 21 – 24.

Figure 1 shows the yearly accumulation of the radio blackout events, with the yearly International Sunspot Number (SILSO) superposed on it as the gray dashed line. For the year 2014 which was the year of SC24 maximum, the number of radio blackouts amounted to 222, consisting of 183 minor (R1), 23 moderate (R2), and 16 strong (R3) events as already shown in Table 1. This is clearly lesser in comparison to previous solar cycles. Figure 2 has showed the number of X-class flares, here solar cycle 24 produced only 49 extreme events, or about a third compared to solar cycle 21 and 22 (~150 extreme events). Also the strength of these flares was lower, with no flares above the X10 level during solar cycle 24. The X9 level flare on 6 September 2017was the strongest flare of the solar cycle 24, standing in the shadow of the spectacular X28 that was observed during solar cycle 23 on 4 November 2003. A 6 X-class flares during the maxima of solar cycle 24 in October 2014 was observed, which was a good result but again a bit meagre compared to the 11 X-class flare event observed during solar cycle 22 in March 1989.

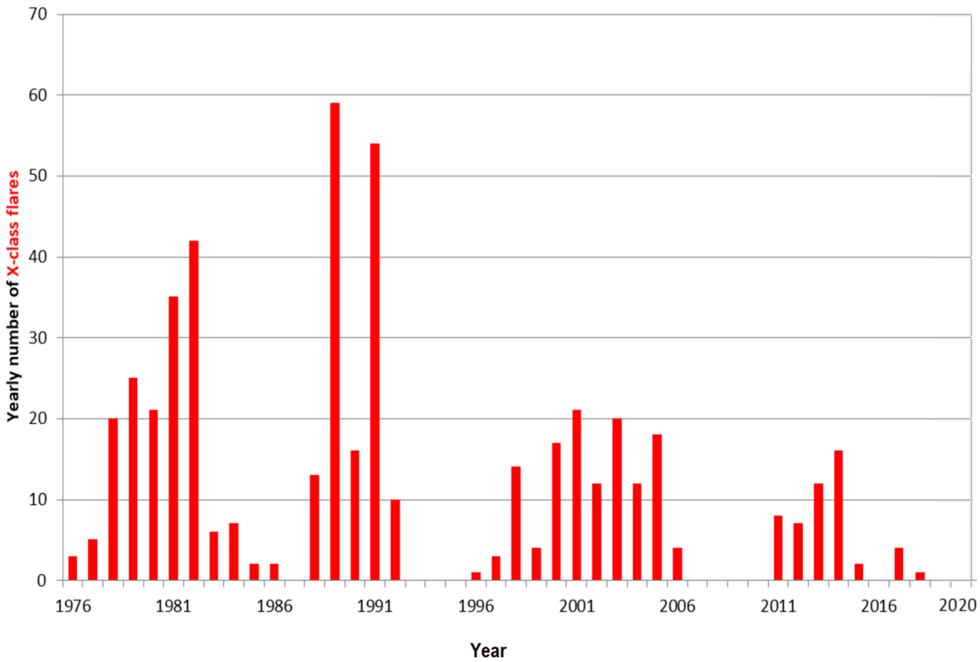

Figure 2. Yearly variation of X class solar flares from 1976 to 2020.

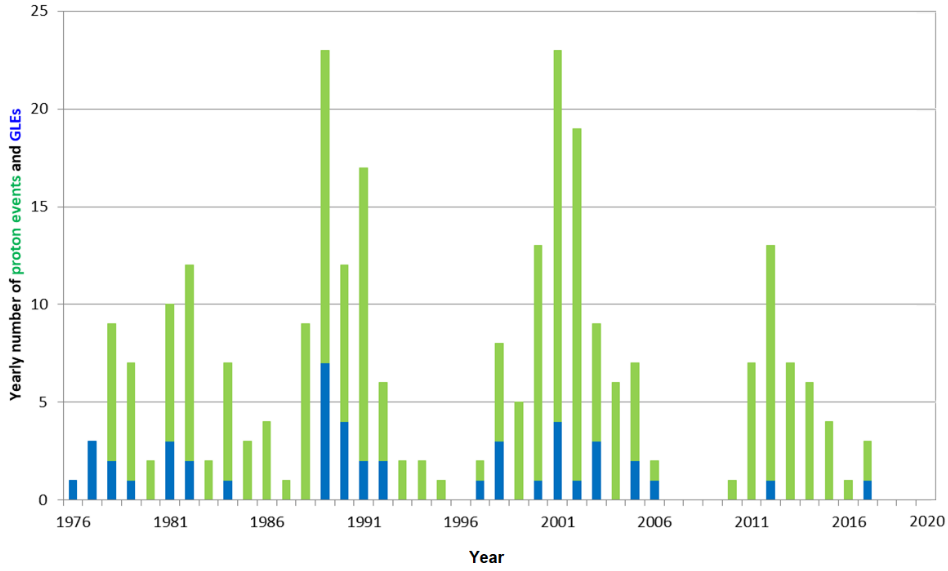

Figure 3. Yearly variation of number of proton events and ground level enhancements for cycles 21 to 24.

Figure 3 has shown the yearly variation of number of proton events for solar cycles 21 to 24. Here the solar cycle 24 has shown relatively well results. The number of events is not that much lower than solar cycle 21 (42 and 59 respectively), and it tops solar cycle 21 when it comes to the intensity (in particle flux units; 1 pfu = particles per square cm per second per steradian) of strongest proton events (6530 pfu vs. 2900 pfu). Solar cycle 22 holds the record of strongest proton event since 1976 (43000 pfu), and solar cycle 23 produced the most proton events in one solar cycle (94, or more than double of what we have seen during solar cycle 24). The solar cycle 24 shows very lower level observations when it comes to ground level enhancements (GLE). These occur during a proton event that is associated with particles having energy well above the regular 10 MeV, rather in the neighbourhood of around 1 GeV (*Gopalswamy et al.*, 2012; *Asvestari et al.*, 2017). When these particles collide with particles in the Earth's upper atmosphere, they can create a shower of secondary particles which can be detected by neutron monitors on ground (*Gopalswamy et al.*, 2012). Several conditions (number of stations, percentage increase above background) need to fulfill before an increase in the observed neutron counts is validated as a genuine GLE (*Mishev and Velinov*, 2018). Since the start of the measurements in the 1940s, only 72 such events have been recorded (*Usoskin et al.*, 2011). For solar cycle 21 to 23, about 13-16 events per solar cycle have been recorded. For solar 24, the count stops at 2: one on 17 May 2012, and the other on 10 September 2017 which was associated with the 2nd strongest flare of solar cycle 24 (X8 level).

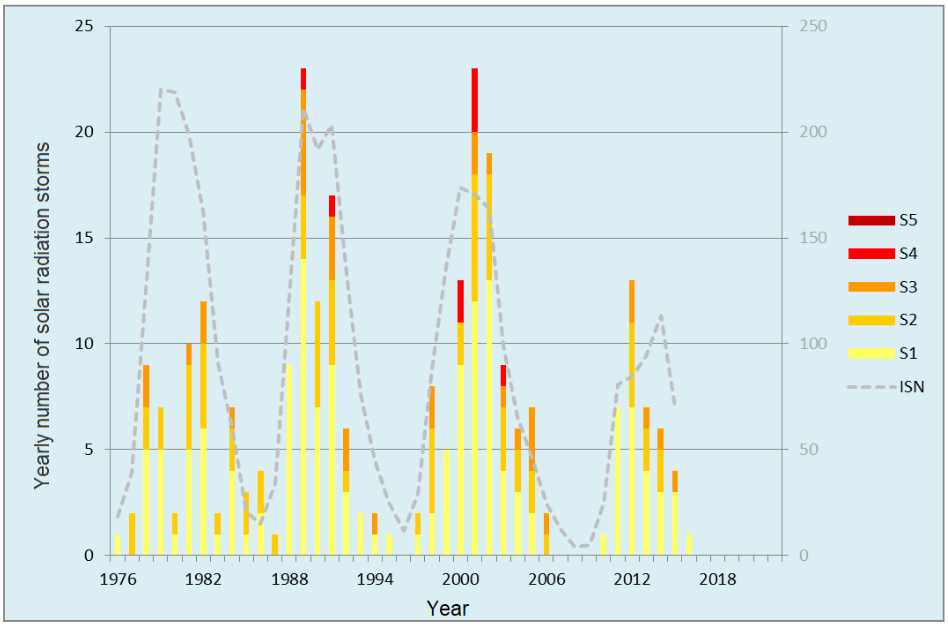

Figure 4. Number of solar radiation storms occurred during solar cycles 21 – 24.

Concerning the number of solar radiation storms (proton storms), it is no surprise that SC24 is again the least active (Figure 4). Interestingly, it is not that much lower in number (39 vs. 59) and intensity (max. S3 events) than SC21 despite the large difference in maximum yearly sunspot number (220 vs. 113). Also remarkable is that 2012 is the year with the most and most intense radiation storms during SC24, and not 2014, the year of solar cycle maximum.

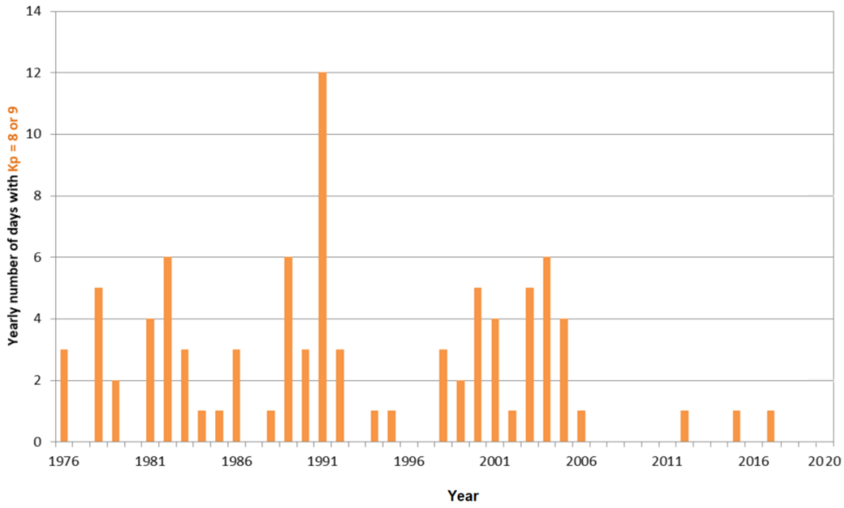

Figure 5. Yearly variation of number of days with Kp = 8 or 9 during 1976 to 2020.

We can see the depressing statistics continue also in case of geomagnetic disturbances. When counting the days with severe or extremely severe geomagnetic disturbances (Kp = 8 or 9), the counter for solar cycle 24 stops already at 3: 9 March 2012, 22 June 2015 and 8 September 2017. So far, no days with Kp= 9 have been recorded during solar cycle 24. For the 3 previous solar cycles, there were always between 27 and 31 days with (extremely) severe geomagnetic disturbances. Figure 5 clearly shows how absent strong geomagnetic activity has been during this solar cycle. Intensity wise, only during the geomagnetic storms of 17 March 2015 and 22 June 2015 reached the Dst index (Disturbance storm-time index) values below -200 nT. The Dst index is often used for gauging the intensity of a geomagnetic storm. Compared to the previous solar cycles, there have been much more intense cases such as on 13-14 March 1989 (Dst = -589 nT) when the province of Québec in Canada experienced a power grid failure that lasted for several hours (*Stauning*, 2013).

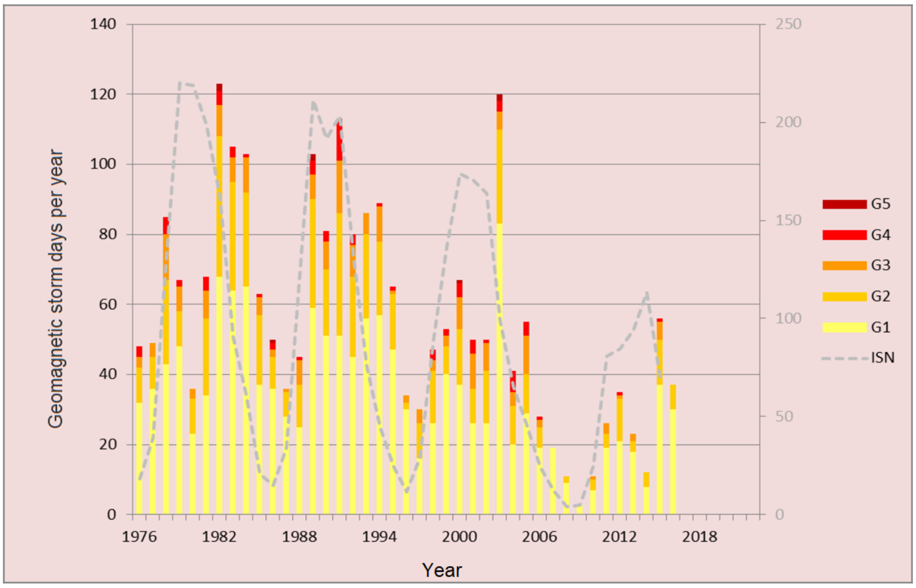

Figure 6. Number of geomagnetic storm days per year during solar cycles 21 – 24.

The plot of the geomagnetic storm days (Figure 6) bears much less resemblance with the evolution of the sunspot number than in the previous two charts given in figures 1 and 4. This is because minor to strong geomagnetic disturbances can also be caused by the high speed solar wind streams (HSS) from coronal holes, hence distorting the familiar outlook of the sunspot cycle. Nonetheless, even then it is very clear that SC24 has been quite disappointing when it comes to the number and intensity of geomagnetic storms, with no extreme storms (G5) so far and precious few severe events (G4). Worse, the numbers even get depressingly low when one compares to other years such as e.g. the 120 storming days in 2003. Interestingly, the number of geomagnetic storm days is peaking in 2015-2016, so after the SC24 maximum in 2014. This is particularly due to the HSS from numerous coronal holes, and is a well-known aspect of this stage of a solar cycle.

Considering the highest solar activity phenomena involving different parameters for each of the four solar cycles 21-24, the highest value of monthly sunspot number was recorded in Jun 1989 (SC 22) which was about 284.5. The highest monthly sunspot area was observed in Feb 1982 (SC 21), which was about 3719.0 MH. The highest monthly 10.7 cm radio flux value (~247.2) was recorded during SC 22 in Jun 1989. The strongest solar flare of type X28 was observed on 4 Nov 2003 (SC 23) while solar cycle 21 have largest number of total number of X class flares. Strongest proton event (43000 MeV; in pfu) was occurred on 24 March 1991 (SC 22) while solar cycle 23 recorded the largest number of such proton events (~94). Here solar cycle 24 has no largest record values at all, this simply indicating that this cycle was a weakest cycle compared to the three previous ones. So, in every domain solar 24 has been outperformed by its three predecessors. The solar cycle 24 activity is most likely comparable to the solar cycles in the late 19^{th} and early 20^{th} century, but most of the above mentioned parameters were not available at that time, preventing definite conclusions.

The correlation coefficients for various solar activity parameters from solar cycle 21 to 24 have been calculated in the study. The statistical analysis and numerical calculated values presented in study implies that the SSN and F 10.7 cm solar index, Lyman alpha index and Mg II index was highly correlated and the correlation coefficient is high ($\geq$ 0.9) for solar cycles 21 to 23 and was ~0.7, 0.8 and 0.9 for solar cycle 24 respectively. Therefore for any correlative study any one of these parameters can be used for finding the solar terrestrial relationship. The correlation coefficient between SSN and Ap index was not as high as found between the SSN and F 10.7 cm index. The correlation coefficient is ~0.384 (highest) for solar cycle 22 and the lowest (~0.112) for solar cycle 24. Anti-correlation between SSN and cosmic ray intensity were almost similar for solar cycles 21 and 24 (–0.810 and –0.895) and –0.639 (lowest) for solar cycle 23. The correlation coefficients between SSN and number of solar flares (M+X) were high during the period of solar cycles 21, 22 and 23 ($\geq$ 0.90) and ~0.845 for solar cycle 24 yields the lowest correlation coefficient. We have found that the peak values of CMEs rate were large for odd cycles (21 and 23) in comparison to even cycles (22 and 24). The correlation coefficient between SSN and CMEs occurrence rate were maximum for solar cycle 21 and 22 (0.945 and 0.972). For solar cycle 24 this correlation was weakest (0.871).

4. Conclusions

Understanding the complex nature of solar cycle remains one of the most important issues in solar physics. In this study several key parameters of the solar cycles have been analysed. Summary of highest solar activity phenomena involving various parameters for each of the four solar cycles (21 to 24) have been presented. The highest value of sunspot number among all the solar cycles was observed during solar cycle 22 and the largest monthly sunspot area was witnessed during solar cycle 21. Highest monthly value of 10.7 cm radio flux (1 AU; in sfu) was recorded during solar cycle 22. The most extreme solar flare of the level of X 28 was occurred in solar cycle 23 and the largest number of such extreme flares was observed during solar cycle 21. The Strongest proton event (>10 MeV) was witnessed in solar cycle 22 and largest sun of these strongest proton events was recorded in solar cycle 23. Solar cycle 23 witnessed the largest number of ground level enhancements (GLE) while solar cycle 21 witnessed the strongest geomagnetic storm.

We found out the correlation coefficients of linear regression for F 10.7 cm index, Lyman alpha index, Mg II index, cosmic ray intensity, number of extreme flares and CMEs rate versus SSN during solar activity cycles 21, 22, 23 and 24. We showed that correlation sunspot number and F 10.7 cm index was highest during solar cycle 21 and during solar cycle 24 its value was lowest. The correction of sunspot number and Lyman alpha index was also highest during solar cycle 21 and lowest during solar cycle 24. In case of the correlation of sunspot number versus Mg II index solar cycle 22 got the highest value of correlation coefficient while solar cycle 24 was assigned lowest value. The correlation between sunspot number and cosmic ray showed some interesting results, here the value of anti-correlation was highest for solar cycle 24 and it was lowest for solar cycle 23. Perhaps the correlation coefficient between sunspot number and Ap index was small for each of the four solar cycles but it was highest in case of solar cycle 22 and lowest in case of cycle 24. The correlation between Sunspot Number and number of M-class and X-class flares was highest during solar cycle 21 and it was lowest in case of solar cycle 24. The CMEs occurrence rate showed high correlation with sunspot number in solar cycle 23 and it was lowest in case of solar cycle 24. From discussions, we can observe that solar cycle 24 has no red text at all, this simply indicating that this solar cycle was a weakest in every domain compared to the three previous solar cycles. The solar cycle 24 activity is most likely comparable to the solar cycles 12 and solar cycle 14 observed in the late 19^{th} and early 20^{th} century. This may be an indication that, in particular, all observed indices are approaching to the “Quiet Sun Level”.

References

Asvestari E., Willamo T., Gil A., Usoskin I.G., Kovaltsov G.A., Mikhailov V.V., Mayorov A., 2017. Analysis of Ground Level Enhancements (GLE): Extreme solar energetic particle events have hard spectra. Adv. Space Res., 60, 781-787.

Bhargawa A., Singh A.K., 2021. Elucidation of some solar parameters observed during solar cycles 21 – 24**.** Adv. Space Res., https://doi.org/10.1016/j.asr.2021.04.037

DeLand M.T., Cebula R.P., 1994. Comparisons of the Mg II index products from the NOAA- 9 and NOAA-11 SBUV/2 instruments. Sol. Phys., 152, 61–68.

Egorova T., Rozanov E., Manzini E., Haberreiter M., Schmutz W., Zubov V., Peter T., 2004. Chemical and dynamical response to the 11-year variability of the solar irradiance simulated with a chemistry-climate model. Geophys. Res. Lett., 31, L06119.

Gaidash S.P., Belov A.V., Abunina M.A., et al., 2017. Space Weather Forecasting at IZMIRAN. Geomagn. Aeron., 57, 869–876.

Goode P.R., Pallé E., 2007. Shortwave Forcing of the Earth's Climate: Modern and Historical Variations in the Sun's Irradiance and the Earth's Reflectance. J. Atmospheric Sol. Terr. Phys., 69, 1556-1568.

Gopalswamy N., Xie H., Yashiro S., Akiyama S., Makela P., Usoskin I.G., 2012. Properties of ground level enhancement events and the associated solar eruptions during solar cycle 23. Space Sci. Rev., 171, 23–60.

Gulyaeva T.L., Gulyaev R.A., 2020. Chain of responses of geomagnetic and ionospheric storms to a bunch of central coronal hole and high speed stream of solar wind. J. Atmos. Solar Terr. Phys., 208, 105380.

Hanuise C., Cerisier J.C., Auchére F., Bocchialini K., et al., 2006. From the Sun to the Earth: impact of the 27–28 May 2003 solar events on the magnetosphere, ionosphere and thermosphere. Ann. Geophys., 24, 129–151.

Kopp G., Lean J.L., 2011. A new, lower value of total solar irradiance: evidence and climate significance. Geophys. Res. Lett., 38, L01706.

Menvielle M., Iyemori T., Marchaudon A., Nosé M., 2011. Geomagnetic Indices. In: Mandea M., Korte M. (eds) Geomagnetic Observations and Models. IAGA Special Sopron Book Series, vol. 5. Springer, Dordrecht.

Mishev A.L., Velinov P.I.Y., 2018. Ion production and ionization effect in the atmosphere during the Bastille day GLE 59 due to high energy SEPs. Adv. Space Res., 61, 316–25.

Papaioannou A., Sandberg I., Anastasiadis A., et al., 2016. Solar flares, coronal mass ejections and solar energetic particle event characteristics. Journal of Space Weather and Space Climate, 6, A42.

Pesnell D.W., 2020. Lessons learned from predictions of Solar Cycle 24. J. Space Weather & Space Clim., 10, 60.

Roeckner E., Brokopf R., Esch M., Giorgetta M.A., Hagemann S., Kornblueh L., Manzini E., Schlese U., Schulzweida U., 2006. Sensitivity of simulated climate to horizontal and vertical resolution in the ECHAM5 atmosphere model. J. Clim., 19, 3771– 3791.

Singh A.K., Tonk A., 2014. Solar activity during first six years of solar cycle 24 and 23: a comparative study. Astrophys. Space Sci., 353, 367-371.

Singh A.K., Bhargawa A., 2017. An early prediction of 25th solar cycle using Hurst exponent. Astrophys. Space Sci., 362, 199.

Singh A.K., Bhargawa A., 2019. Prediction of declining solar activity trends during solar cycles 25 and 26 and indication of other solar minimum. Astrophys. Space Sci., 364, 12.

Singh A.K., Bhargawa A., 2020. Ascendancy of Solar Variability on Terrestrial Climate: A Review. Journal of Basic & Applied Sciences, 16, 105-130.

Stauning P., 2013. Power grid disturbances and polar cap index during geomagnetic storms. J. Space Weather Space Clim., 03, A22.

Turner J., Hosking J.S., Phillips T., Marshall G.J., 2013. Temporal and spatial evolution of the Antarctic sea ice prior to the September 2012 record maximum extent. Geophys. Res. Lett., 40, 5894–5898.

Usoskin I.G., Kovaltsov G.A., Mironova I.A., Tylka A.J., Dietrich W.F., 2011. Ionization effect of solar particle GLE events in low and middle atmosphere. Atmos. Chem. Phys., 11, 1979–1988.

White O.R., de Toma G., Rottman G.J., Woods T.N., Knapp B.G., 1998. Effects of spectral resolution on the Mg II index as a measure of solar variability. Sol. Phys., 177, 89–103.